

Supplementary material

Effects of CO₂ to deactivation behaviors of Co/Al₂O₃ and Co/SiO₂ for CO hydrogenation to hydrocarbons

Kyung Soo Park, K. Saravanan, Seon-Ju Park, Yun-Jo Lee, Ki-Won Jeon, Jong Wook

Bae*

Figure S1. Pore size distribution of the fresh Co/ γ -Al₂O₃ and Co/SiO₂ catalysts

Figure S2. PXRD patterns of the fresh Co/ γ -Al₂O₃ [from **ref. 8**] and Co/SiO₂ catalysts

Figure S3. H₂-TPR profiles of the fresh Co/ γ -Al₂O₃ and Co/SiO₂ catalysts at a heating rate of 5 °C/min from 100 to 1100 °C

Figure S4. XPS analysis of (A) Al 2p of the Co/ γ -Al₂O₃ and (B) Si 2p of the Co/SiO₂ on the fresh (only reduction), used catalysts after FTS reaction without CO₂ addition and used catalysts after FTS reaction with 20%CO₂ addition

Figure S5. Schemes of FT-IR analyses for the successive adsorption of CO \rightarrow CO₂ \rightarrow CO on the reduced CoAl and CoSi after H₂ purge at each step to verify the oxidation-reduction properties of the supported cobalt nanoparticles

Figure S6. FT-IR analysis of adsorbed CO molecules on the (A) Co/ γ -Al₂O₃ catalyst and (B) Co/SiO₂ catalyst for the fresh catalyst, used catalyst without CO₂ addition and used catalyst with CO₂ addition

Figure S7. CO conversion and product distribution with time one stream on the (A) Co/ γ -Al₂O₃ without CO₂ addition, (B) Co/ γ -Al₂O₃ with 20vol%CO₂ addition, (C) Co/SiO₂ without CO₂ addition and (D) Co/SiO₂ with 20vol%CO₂ addition

Figure S8. Cobalt particle size distributions from the TEM images of (A) Co/ γ -Al₂O₃, (B) Co/SiO₂: (1) reduced catalyst, (2) used catalyst without CO₂ addition and (3) used catalyst with CO₂ addition

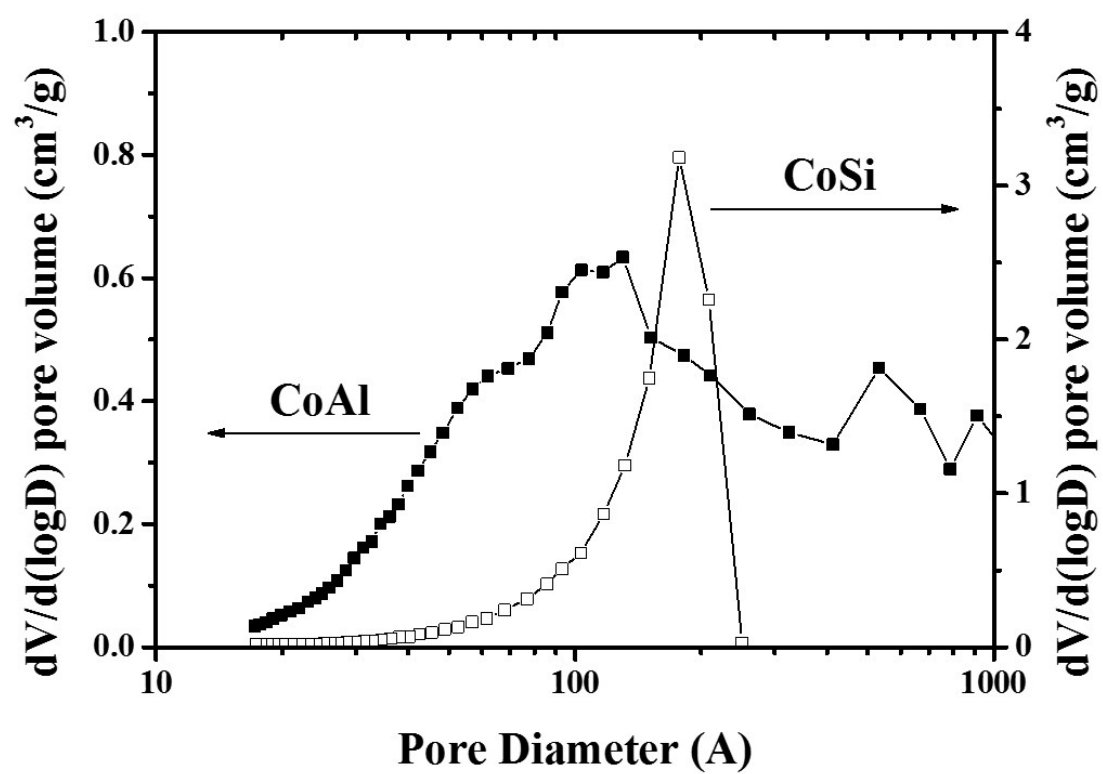


Figure S1. Pore size distribution of the fresh Co/ γ -Al₂O₃ and Co/SiO₂ catalysts

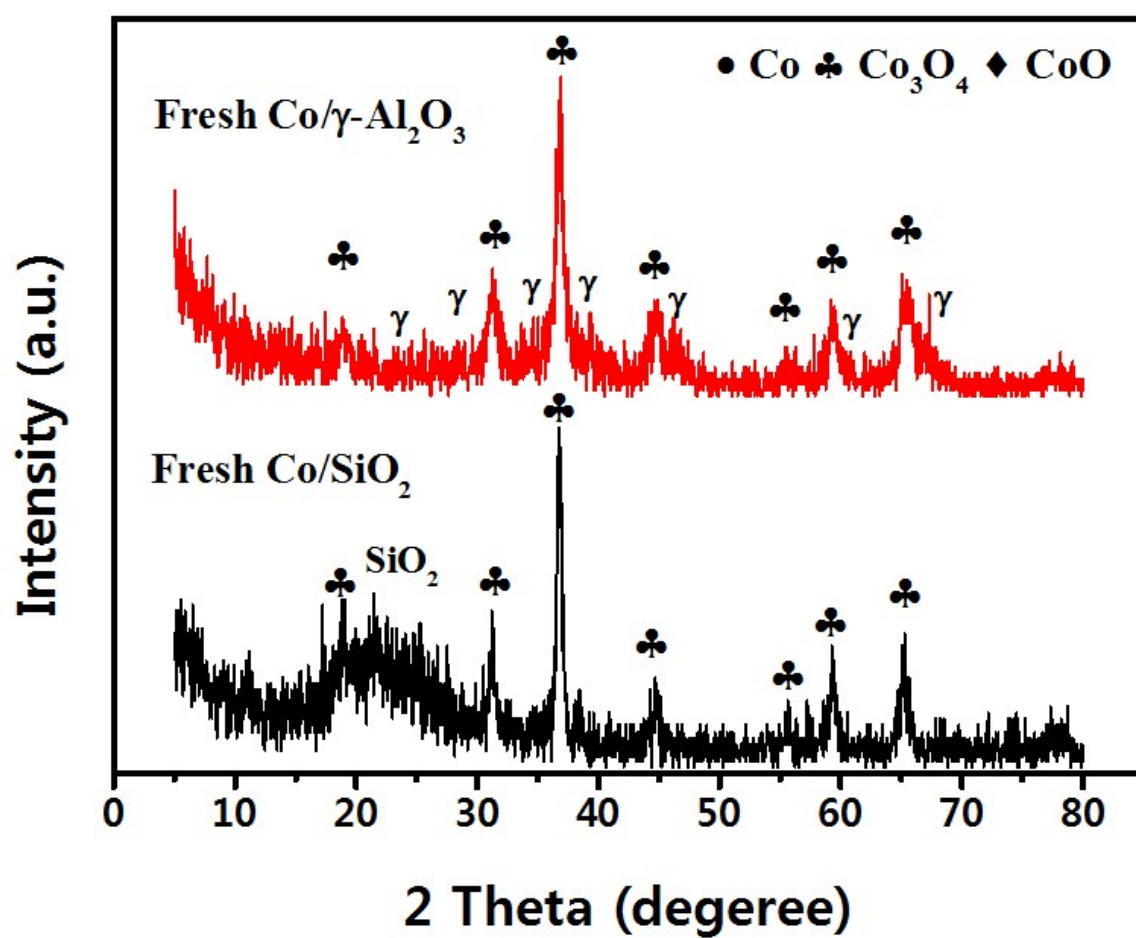


Figure S2. PXRD patterns of the fresh Co/ $\gamma\text{-Al}_2\text{O}_3$ [from ref. 8] and Co/ SiO_2 catalysts

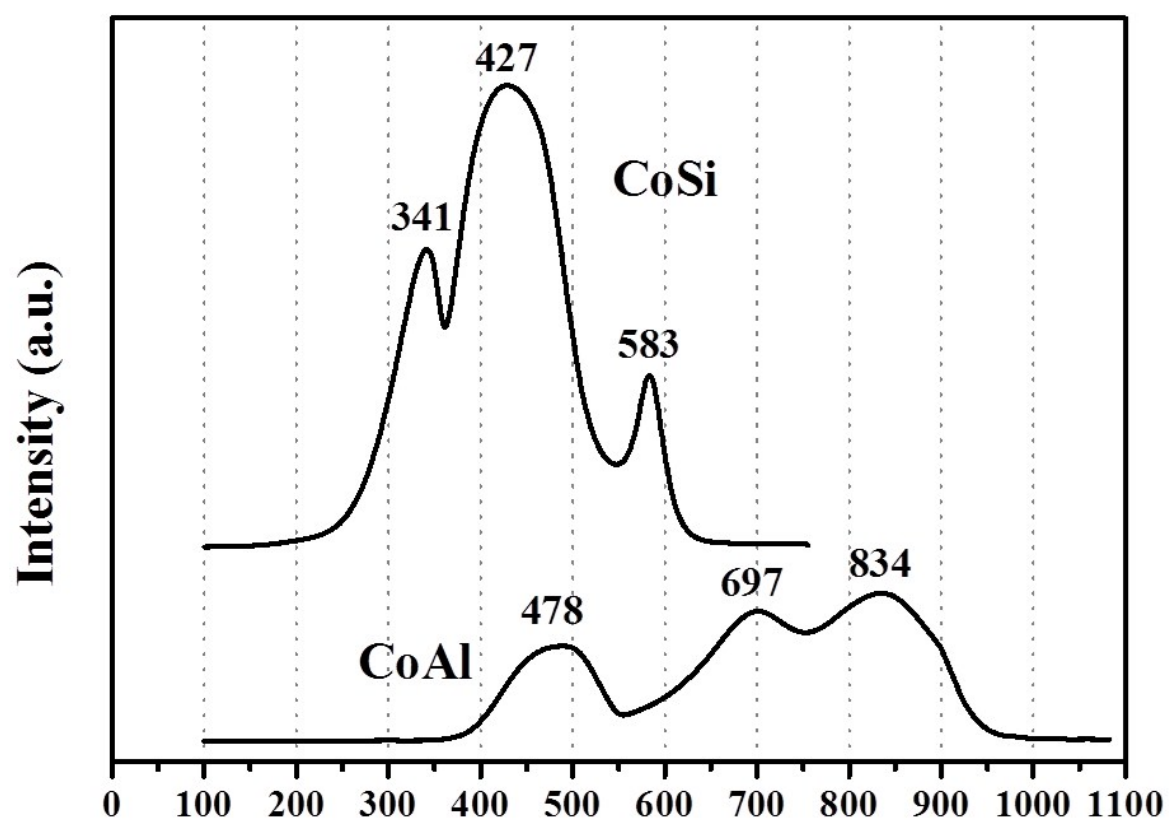


Figure S3. H₂-TPR profiles of the fresh Co/ γ -Al₂O₃ and Co/SiO₂ catalysts at a heating rate of 5 °C/min from 100 to 1100 °C

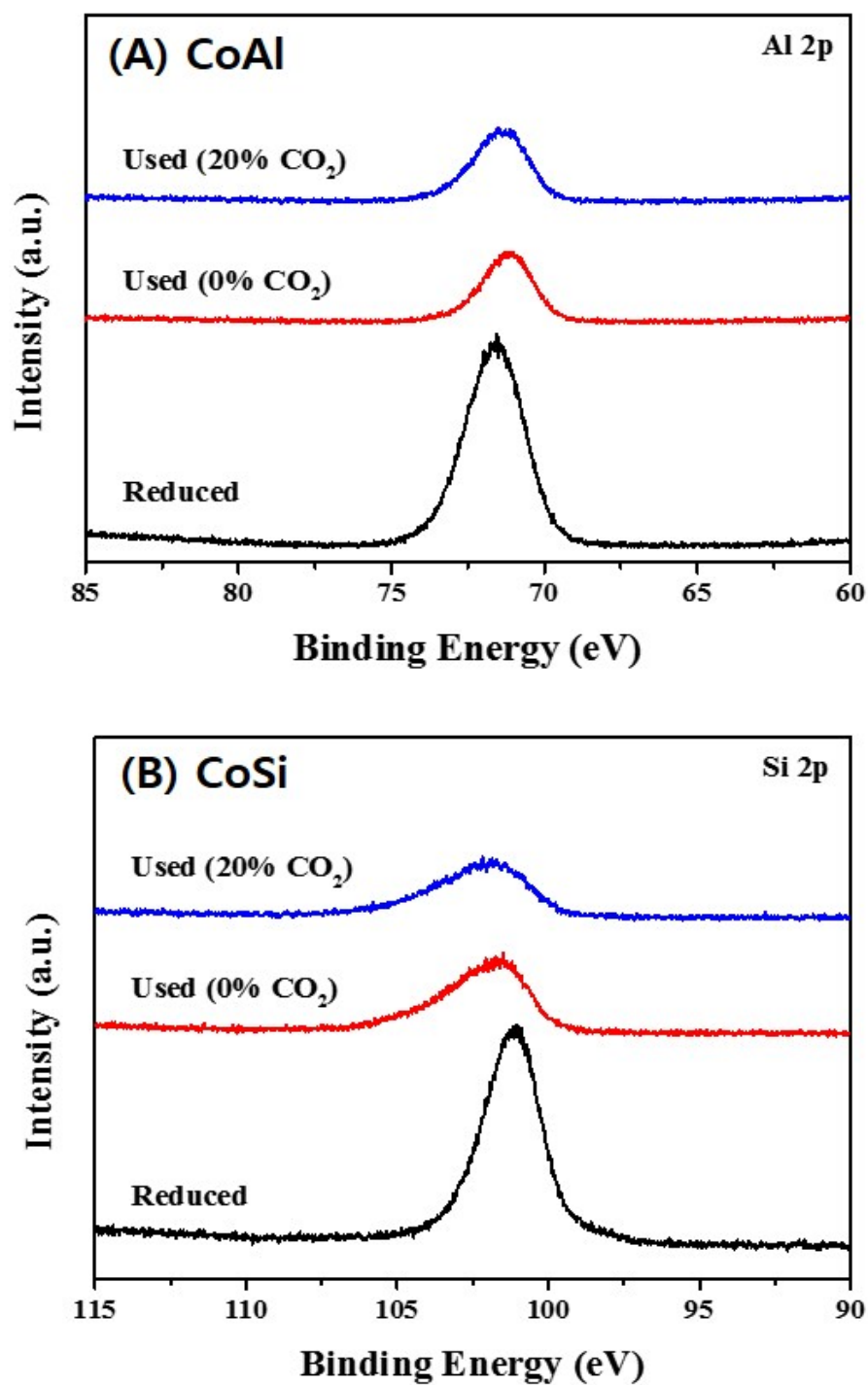


Figure S4. XPS analysis of (A) Al 2p of the Co/ γ -Al₂O₃ and (B) Si 2p of the Co/SiO₂ on the fresh (only reduction), used catalysts after FTS reaction without CO₂ addition and used catalysts after FTS reaction with 20%CO₂ addition

In-situ FT-IR analysis schemes on the CoAl and CoSi

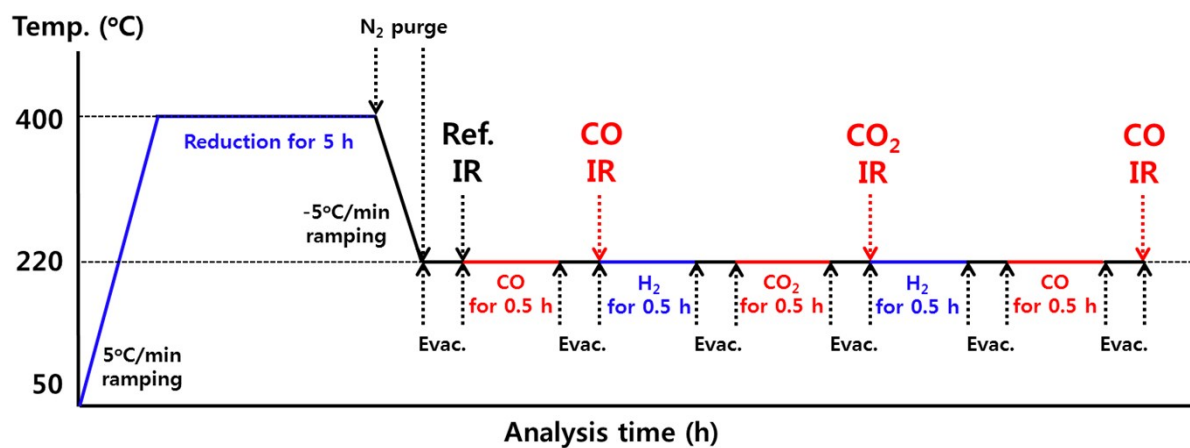


Figure S5. Schemes of FT-IR analyses for the successive adsorption of CO → CO₂ → CO on the reduced CoAl and CoSi after H₂ purge at each step to verify the oxidation-reduction properties of the supported cobalt nanoparticles

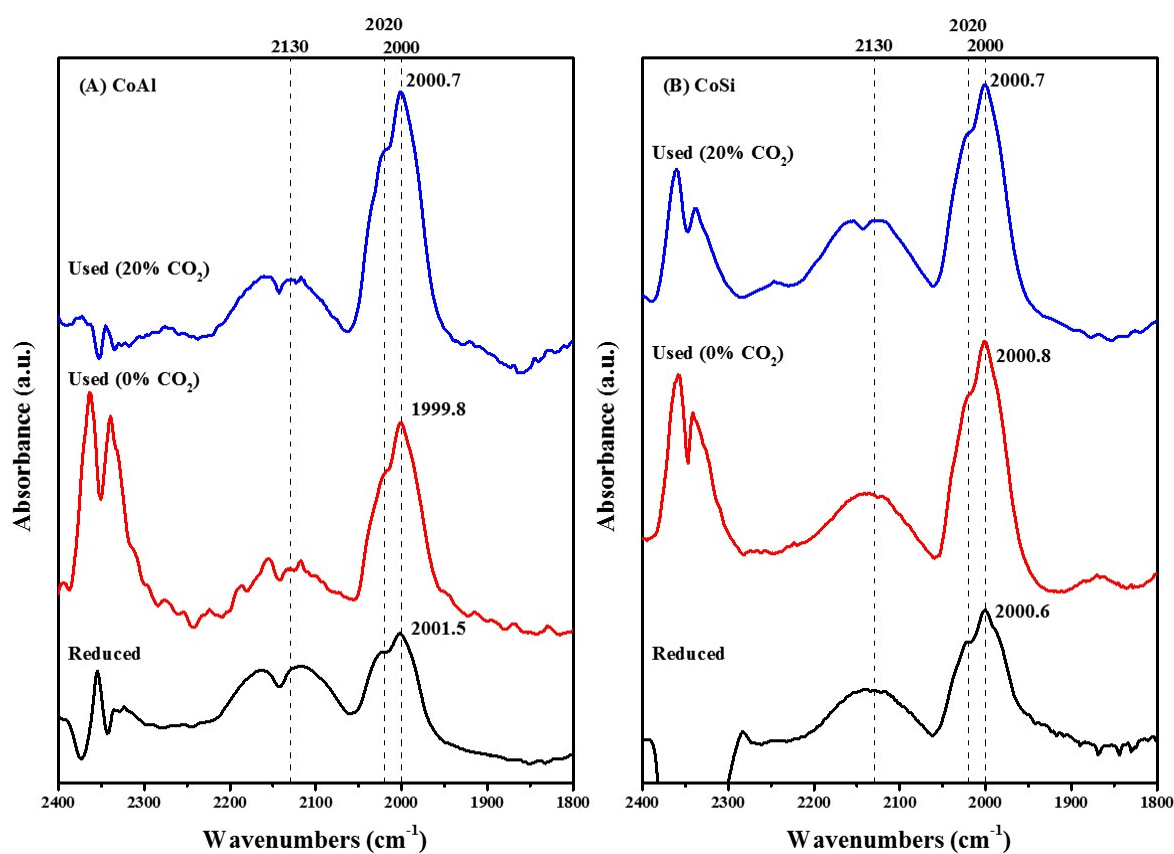


Figure S6. FT-IR analysis of adsorbed CO molecules on the (A) Co/ γ -Al₂O₃ catalyst and (B) Co/SiO₂ catalyst for the fresh catalyst, used catalyst without CO₂ addition and used catalyst with CO₂ addition

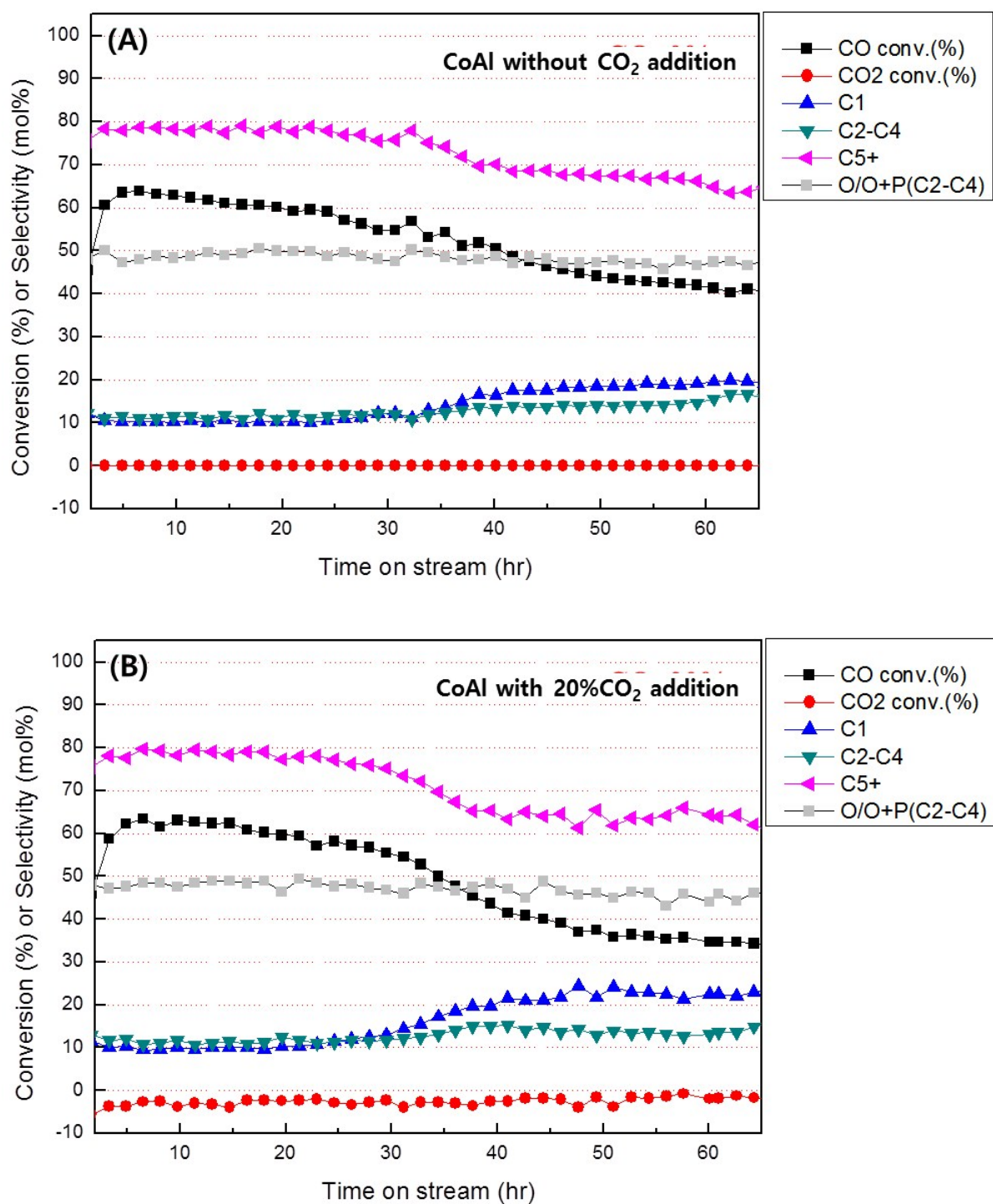


Figure S7. CO conversion and product distribution with time on stream on the (A) Co/ γ -Al₂O₃ without CO₂ addition, (B) Co/ γ -Al₂O₃ with 20vol%CO₂ addition, (C) Co/SiO₂ without CO₂ addition and (D) Co/SiO₂ with 20vol%CO₂ addition

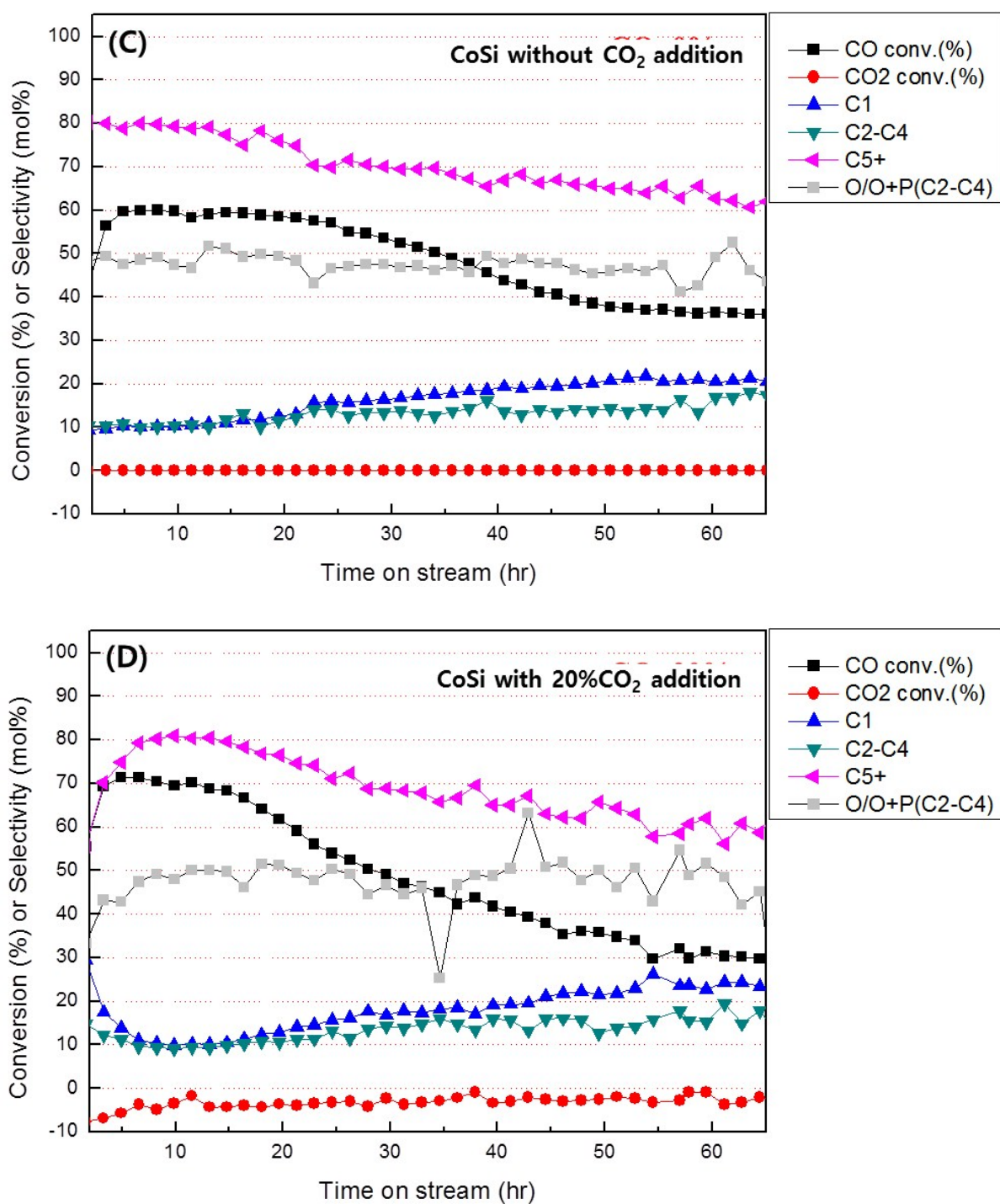


Figure S7. CO conversion and product distribution with time on stream on the (A) Co/ γ -Al₂O₃ without CO₂ addition, (B) Co/ γ -Al₂O₃ with 20vol%CO₂ addition, (C) Co/SiO₂ without CO₂ addition and (D) Co/SiO₂ with 20vol%CO₂ addition (continued)

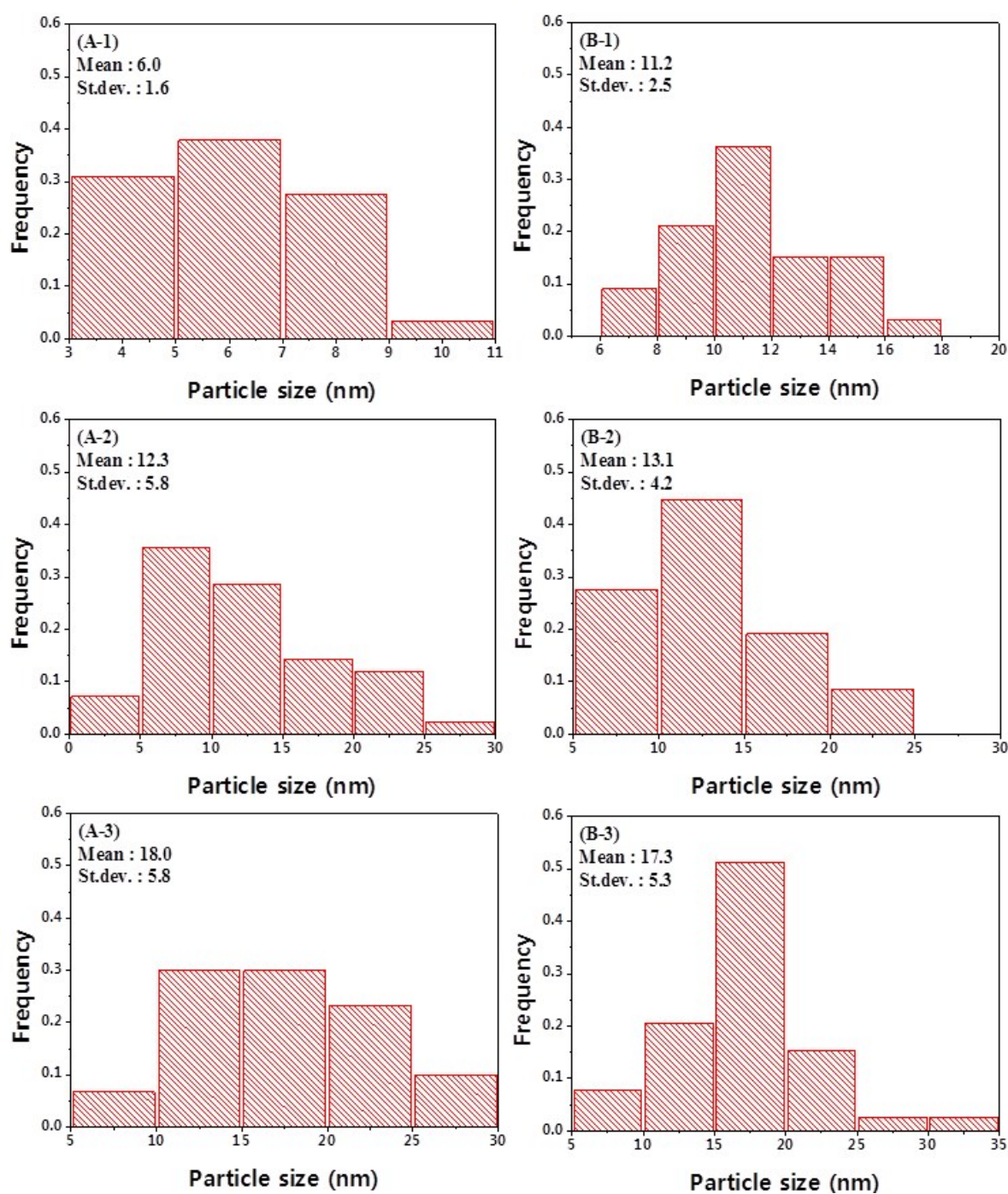


Figure S8. Cobalt particle size distributions from the TEM images of (A) Co/ γ -Al₂O₃, (B) Co/SiO₂: (1) reduced catalyst, (2) used catalyst without CO₂ addition and (3) used catalyst with CO₂ addition